Development of a Meso-scale Dual-axis Steel Accelerometer with Hall-effect Sensors

Sambuddha Khan, P. Muddukrishna and G. K. Ananthasuresh

Abstract

We present here an overview of the work done on the development of a meso-scale dual-axis spring steel in-plane accelerometer equipped with Hall-effect sensors. The design of the accelerometer has the unique feature that there is perfect de-coupling of the motions in the two in-plane orthogonal directions. One more extra feature is the use of rechargeable Li-ion batteries as a part of the proof-mass in addition to serving as the power source. The mechanical element of the accelerometer is made of EN J42/AISI 1080 spring steel foil machined using Wire-cut Electro-Discharge Machining (EDM) process. Allegro A1395 linear Hall-effect sensors are used to transduce the displacement of the proof-mass into voltage. The packaged sensor has an overall dimension of $73\ \text{mm} \times 73\ \text{mm} \times 28.5\ \text{mm}$. The packaged sensor can detect an acceleration signal as small as 25 milli-g with a measured sensitivity of 78 mV/g and 102 mV/g along X and Y axes respectively. Reason for asymmetry and scope for improvement in performance, reduction in size, and batch production are also discussed in this paper.

Keywords: Accelerometer, meso-scale, dual-axis, Hall-effect sensor, mechanism and Wire-cut EDM

1 Introduction

Accelerometers are one of the most widely used sensors today because of their importance in many devices and the availability of different manufacturing technologies and batch-fabrication processes. Miniaturized sensors are becoming popular because of their low cost and uncompromised performance as compared to their macro counterparts. Silicon micromachining is one of the most widely used manufacturing technologies that enable miniaturization of sensors such as accelerometers, gyroscopes, etc. without compromising their performance. Many applications that use micromachined accelerometers require low to medium resolution of the order of $\text{milli-g}/\sqrt{\text{Hz}}$ (milli-g means one thousandth of the acceleration due to gravity, i.e., $10^{-3} \times 9.81\ \text{m/s}^2$) or better resolution. Commercially available micro-machined milli-g accelerometers are inexpensive but the micro-g accelerometers are very expensive as they require both sophisticated and expensive fabrication technology and transduction techniques. (e.g., tunnelling current-based [1]-[3] and laser interferometry based [4, 5]) that are not suitable for

Sambuddha Khan
Multi-disciplinary and Multi-scale Device and Design (M2D2) Laboratory, Department of Mechanical Engineering, Indian Institute of Science, Bangalore-560012, E-mail: sambud@mecheng.iisc.ernet.in.

P. Muddukrishna
Multi-disciplinary and Multi-scale Device and Design (M2D2) Laboratory, Department of Mechanical Engineering, Indian Institute of Science, Bangalore-560012,E-mail: krishepm@mecheng.iisc.ernet.in.

G. K. Ananthasuresh
Multi-disciplinary and Multi-scale Device and Design (M2D2) Laboratory, Department of Mechanical Engineering, Indian Institute of Science, Bangalore-560012, E-mail: suresh@mecheng.iisc.ernet.in.

light-weight and portable applications. The other relatively simple transduction techniques such as capacitive [6]-[10], piezoelectric [11, 12] piezoresistive [13]-[15] and resonant [16]-[19] require high precision and expensive signal conditioning circuitry to be integrated to the mechanical part of the sensor.

Even though the packaged accelerometers are themselves very small, they often require evaluation boards, battery or external power supply, and mountings that make them big. A pertinent question that becomes the premise for this paper is: why cannot materials and manufacturing techniques from the macro domain be scaled down? Silicon is a good mechanical material at the micro scale, but steel is an excellent material at macro scale. In this paper, we explore steel as a mechanical material at the meso-scale.

Meso-scale, for the purpose of this paper, refers to the size between macro scale (few cm to meter) and micro scale (0.1 μm to a few mm). In such a meso-scale range (100s of μm to a cm), the choice of materials changes; silicon is no more the choice material because it cannot be made bigger than a few mm in plane while its thickness is severely restricted. The rationale for going for meso-scale sensor element is that packaged silicon-based micro-machined devices are anyway going to have a size compatible with the meso-scale when they come with their signal conditioning evaluation board. So, making the sensor element up to 10 times bigger does not compromise the size of the packaged sensor. The advantages are in cost even when the volume of market is low. This is because expensive clean-room environment is not necessary. The material needed is also cheap. Metals are good candidates. In this work, we used EN J42/AISI 1080 spring steel. Manufacturing techniques are derived from macro-scale manufacturing method. We chose Wire-cut Electro-Discharge-Machining (EDM) in this work. Eventually, batch fabrication can also be done using punching and thus the economic advantage can be achieved.

Based on the foregoing, in this paper, we propose an inexpensive and simple dual-axis meso-scale accelerometer made of spring steel for low-g medium-resolution applications. It is an extension of our earlier work [20] in which we had presented a single-axis accelerometer made of spring steel. It had two embodiments, one with Hall-effect sensing and another with capacitive sensing. With these two sensing modes, it had a resolution of 14 mg and 1 mg resolution, respectively. The current paper extends that work to measuring acceleration in two in-plane axes simultaneously. The design of the accelerometer, in principle, has the unique feature of perfect de-coupling of motions in the two in-plane orthogonal directions. A de-coupling mechanism is used as the inertial unit comprising both the proof-mass and the suspension.

In this work, Hall-effect based proximity sensors are used for signal conditioning. The Hall-effect sensors also require external DC power supply to operate. For this purpose, rechargeable Li-ion batteries are used as the in-built power sources to the Hall-effect sensors; they are also used as part of the proof-mass of the accelerometer.

2 A Meso-scale Dual-axis Accelerometer

In this section, the development of a meso-scale dual-axis spring steel accelerometer is presented. The design of the dual-axis accelerometer is discussed followed by the prototyping of the device. The finite element simulation of the mechanical component of the accelerometer is discussed. The signal conditioning using linear

Hall-effect proximity sensors is also covered in detail. Finally, integration of the signal conditioning circuit with the prototype and packaging of the device are also discussed along with the calibration and testing of the prototype.

2.1 Design

A dual-axis accelerometer is designed to sense acceleration in any arbitrary direction in a plane. This uses a compliant mechanism called a compliant XY flexure for decoupling the input excitation into its X and Y components. This design is based on an XY stage, shown in Fig. (1a), developed by Awtar [21]. Here we use it for the purpose of sensing with required modifications to make it an accelerometer.

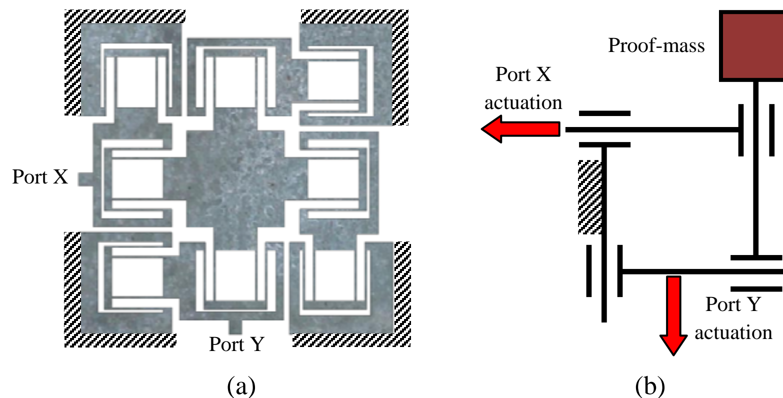

(a) (b)

Figure 1. (a) A parallel arrangement of an XY Stage [21], (b) A schematic diagram showing two independent actuations of a the proof-mass using the XY flexure mechanism [21].

The dual-axis accelerometer requires two independent motions of the proof-mass. The suspensions of the proof-mass are so designed that the proof-mass moves only along the X direction when the device is actuated only along X, and similarly along the Y direction. Actuation of the Port X does not undergo any disturbance when the device is actuated along Y direction and vice versa, as can be seen in the schematic in Fig. (1b). The proof-mass is allowed to move along any arbitrary direction in the plane of the applied acceleration whereas the ports X and Y move by the respective X and Y components of the displacement of the proof-mass in that plane. The schematic of the XY flexure mechanism shows a perfect de-coupling of motions in two in-plane orthogonal directions and thus offers zero cross-axis sensitivity. The modified XY flexure mechanism used in the accelerometer, shown in Fig. (2a) has an overall dimension of 73 mm × 73 mm × 0.5 mm.

The proof-mass is the point of maximum displacement for a conventional single-axis accelerometer. But in this dual-axis accelerometer design, the ports X and Y are the maximum points of displacements along X and Y directions respectively. Thus, the displacement of the proof-mass along X direction can be captured by measuring the displacement at Port X and similarly for Port Y.

Sensitivity is one of the most significant specifications of an accelerometer. The stiffness of the folded beam suspension and the inertia of the proof-mass determine the sensitivity of an accelerometer. Thus, for a given suspension geometry, the

sensitivity can only be improved by increasing the mass of the proof-mass. In this current work, we have enhanced the sensitivity of the accelerometer by attaching spring steel blocks and Li-ion batteries to the accelerometer proof-mass and thus increasing the inertia of the accelerometer. The isometric view and the side view of the solid model of the device, made in SolidWorks [22], are shown in Fig. (2c-d) respectively.

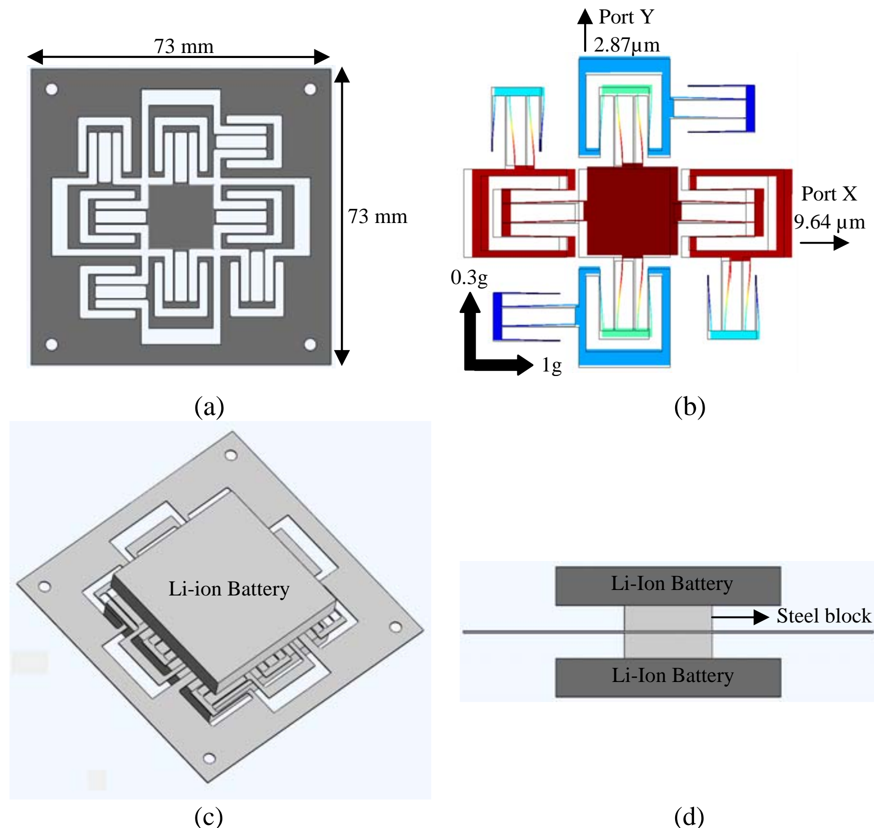

Figure 2. (a) Modified XY flexure used as a dual-axis accelerometer, (b) FE simulation showing the XY flexure mechanism de-coupling two different input accelerations along its X and Y axes, (c) Isometric view of the proposed device with two Li-ion batteries attached to the top and bottom of the metal proof-mass, (d) Side view of the proposed device showing the arrangement to increase the proof-mass using Li-ion batteries and steel blocks.

2.2 Finite element analysis of the design

Finite element analysis was performed using COMSOL Multiphysics software [23] on both the 2D and 3D models of the designed device. Initially, static geometrically nonlinear, elastic analysis was performed by applying the inertial force as a body force on the mechanism without the extra proof-mass due to batteries. As can be seen in Fig. (2b), the mechanism used for the design is able to de-couple the applied acceleration such that Ports X and Y move according to the axial component of the applied force along the X and Y axes. The cross-axial coupling is simulated to be

approximately 0.6 % of the axial displacement which is quite good for an accelerometer application. The modal and frequency response analysis were also performed on the 3D model of the accelerometer along with the steel blocks and the batteries acting as the extra proof-mass. The displacement characteristics is the same for ports X and Y as the structure is geometrically symmetric along both the X and Y axes. The 3 dB bandwidth of the device was simulated to be 20 Hz whereas the natural frequency is around 36.3 Hz. The simulated frequency response (without damping) of the 3D model is shown in Fig. (6b).

2.3 Prototyping

The designed meso-scale dual-axis spring steel accelerometer is fabricated using Wire-cut Electro-Discharge-Machining (Mechanica, Maxicut[e]). The minimum feature that can be fabricated using this machine is 0.2 mm whereas the minimum possible gap between two structures is 1.5 mm. A 0.5 mm thick spring steel (EN J42/AISI 1080) foil was machined using Wire-cut EDM to fabricate the shape of the accelerometer. Several holes were drilled prior to Wire-cut EDM in order to thread the wire through the metal foil.

Two 2 mm thick steel blocks were cut in the size of the proof-mass using a CNC machine and were attached to the top and bottom surface of the proof-mass on the accelerometer. The dimension of each of the steel block added to the existing proof-mass is 15.625 mm × 15.625 mm × 2 mm. In order to attach Li-ion batteries of size 40.78 mm × 40.06 mm × 5.7 mm to the proof-mass, two acrylic cases, serving as the housing for the batteries, were made using the CNC machine and attached to the free surfaces of the top and bottom metal blocks. The attached batteries are elevated by 2 mm from the de-coupling mechanism using those two 2 mm thick steel blocks and become a part of the proof-mass. Thus, the batteries are detachable from of the proof-mass and can be replaced after recharge whenever required.

2.4 Signal conditioning

As discussed in the Section 2.1, the displacements of ports X and Y indicate the inertial force felt by the proof-mass due to the applied acceleration along both X and Y directions. In this paper, linear Hall-effect proximity sensors (Allegro A1395) were chosen to sense the displacements of ports X and Y. The working principle of a Hall-effect sensor is that a potential difference arises across an electrical conductor, transverse to the direction of the current in the conductor when the magnetic field is perpendicular to the current. This is a contactless proximity sensor. The output voltage of the Hall-effect sensor changes as the magnetic field across the sensor varies.

The linear Hall-effect sensor IC of size 2.0 mm×3.0 mm×0.75 mm with micro-lead package (MLP/DFN) [24] and commercially available Neodymium (NdFeB) disc magnets, shown in Fig (3a), with 3 mm diameter and 1.5 mm thickness are used in this work for displacement-sensing. The disk magnets were attached to the ports X and Y of the de-coupling mechanism. A custom designed PCB, shown in Fig. (3b), containing a Hall-effect sensor was attached to the stationary part of the device at a distance of 4.5 mm from the magnet along each X and Y direction. The magnetic field of the disk magnet was measured to be 3100 Gauss and the sensitivity of the Allegro A1395 linear Hall-effect sensor is 10 mV/Gauss. The optimal distance of 4.5

mm was arrived from the calibration curve of the Hall-effect sensor, shown in Fig. (3c), to operate it in a nearly linear region. Finally, the batteries, acting as extra proof-mass, are also connected to the PCBs containing the Hall-effect sensors through wires.

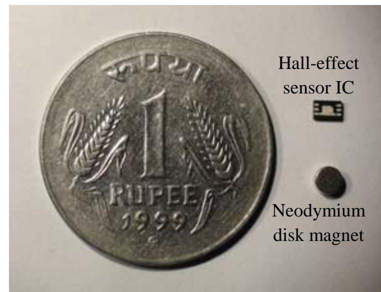

(a)

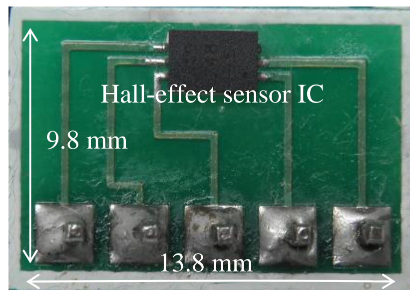

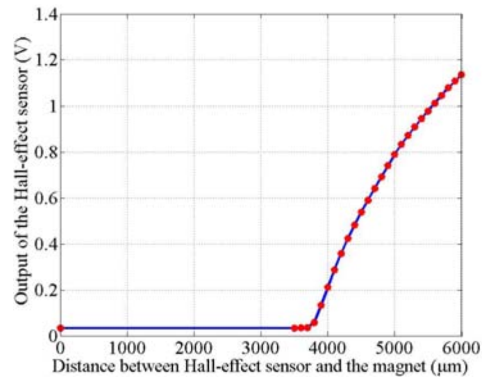

(b) (c)

Figure 3: (a) Linear Hall-effect sensor and the Neodymium disc magnet, (b) Custom PCB with the Hall-effect sensor soldered on it, (c) Calibration curve of the linear Hall-effect sensor used for this work.

2.5 Packaging

An acrylic housing arrangement with top and bottom covers is fabricated using CNC machining for the entire device. The device is placed inside the acrylic housing and the final manual assembly, shown in Fig. (4a-b), is performed using screws. Windows were cut in the housing arrangement to take out the output leads from the PCBs containing the Hall-effect sensors. The overall dimension of the packaged meso-scale spring steel dual-axis accelerometer is 73 mm × 73 mm × 28.5 mm.

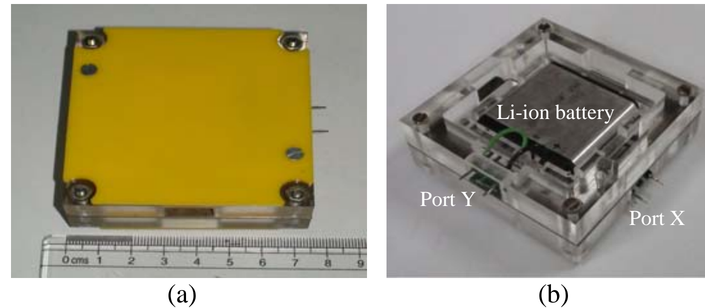

Figure 4: (a) Packaged meso-scale spring steel dual-axis accelerometer with yellow cover and (b) without a cover exposing the top Li-ion battery acting as the extra proof-mass as well as the power source for the Hall-effect sensor at Port Y.

2.6 Calibration and testing

The packaged meso-scale dual-axis spring steel accelerometer was mounted on the LDS shaker table which can vibrate within a specified range of acceleration and frequency. A commercially available 3-axis analog milli-g accelerometer, made of ST Microelectronics (Model: LIS3L02AS4) [25], was used as a reference accelerometer to calibrate the meso-scale dual-axis accelerometer and controlling the shaker table. The experimental setup is shown in Fig. (5).

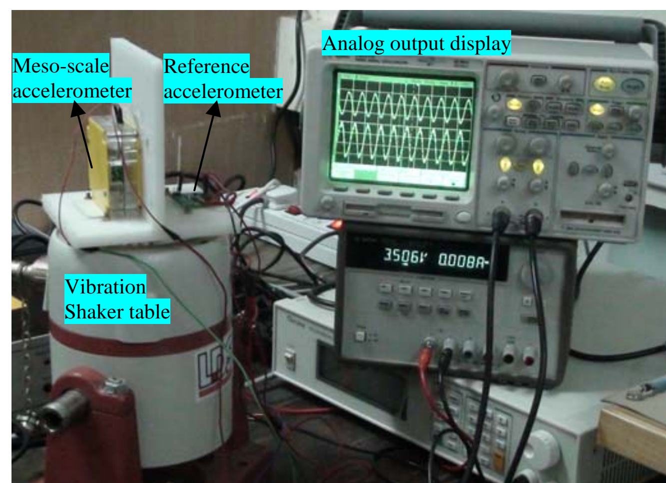

Figure 5: Experimental setup showing the developed sensor being calibrated with respect to a reference accelerometer on a vibration shaker table.

The shaker table along with the device under test was vibrated at different frequencies with an amplitude of vibration of 0.2 g. An oscilloscope was used to record the output of both the axes. The frequency response of the dual-axis accelerometer along the X axis was obtained by plotting the output of the Hall-effect sensor, mounted along the X axis of the accelerometer, with respect to the frequency of the applied acceleration. The experimentally obtained frequency responses for both the X and Y axes are shown in Fig. (6a) with simulation curve superposed on it. The experimentally achieved first two in-plane natural frequencies of the

accelerometer are 39.5 Hz and 52 Hz for X and Y axis respectively whereas the 3 dB bandwidth of the accelerometer is approximately 28 Hz for both the axes. It may be noted that the simulated second natural frequency is 36 Hz.

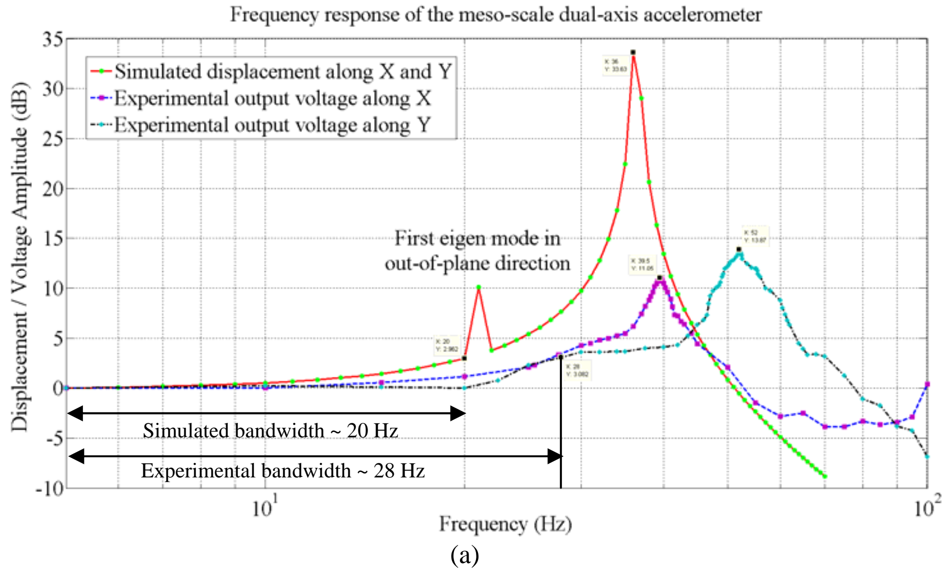

(a)

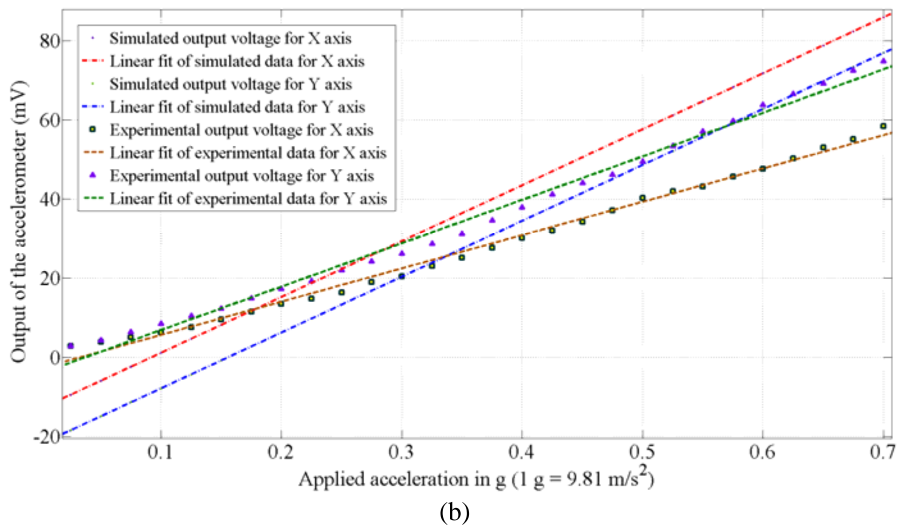

(b)

Figure 6: (a) Plot showing the simulated and experimentally obtained frequency response of the sensor for both X and Y axes, (b) Plot showing experimentally obtained calibration curve of the sensor for both X and Y axes.

The shaker table along with the device under test was again vibrated at different acceleration values varying from 25 milli-g to 0.7 g at a fixed frequency of 10 Hz and the output of the sensor for both X and Y axes was recorded and then plotted to get the calibration curve of the meso-scale spring steel dual-axis accelerometer which is shown in Fig. (6b). The experimentally obtained sensitivity of the

developed accelerometer is 78 mV/g and 102 mV/g approximately for X and Y axes respectively with a minimum detectable acceleration of 25 milli-g for both the axes. Also shown in Fig. (6b) are the linear fits to the simulated data. It can be seen that simulation shows a sensitivity of about 140 mV/g. This discrepancy between simulation and experiment is primarily due to the packaging, the casing that holds the batteries in particular. It is suspected that this is also the reason for the asymmetric experimental data in the X and Y axes.

The off-axial sensitivity was also measured by applying an off-axial load on the device under test and measuring the output of the sensor with respect to the output of the sensor when an axial loading is applied. The off-axial sensitivity is generally expressed in terms of % of the axial sensitivity. The off-axial sensitivity of this accelerometer was measured to be 13.09 % and 12.08 % for X and Y axis respectively.

3 Discussion and Closure

In this paper, we described a meso-scale dual-axis accelerometer made of spring steel and equipped with linear Hall-effect sensors. The accelerometer uses a modified XY flexure mechanism for de-coupling the input excitations in a plane. The accelerometer was fabricated by cutting a 0.5 mm thick spring steel foil using Wire-cut EDM. Two 40.78 mm × 40.06 mm × 5.7 mm Li-ion batteries, used for the power sources of the Hall-effect sensor, are also used as added proof-mass of the accelerometer. Hence, the prototype of the accelerometer does not require any external power supply to operate. The final assembly of the parts of the accelerometer was performed manually and thus misalignment could not be avoided. The prototype was mounted on a shaker table and then tested and calibrated with respect to a reference accelerometer. It was observed that the accelerometer does not have similar characteristics along both the axes because of misalignment during manual assembly, asymmetry in the battery dimension and unequal distance between the moving disk magnet and the Hall-effect sensor IC in both the X and Y axes. The experimentally observed in-plane natural frequency is at 39.5 Hz for X axis and 52 Hz for Y axis where as the 3 dB bandwidth is obtained at 28 Hz approximately for both the axes. The sensitivity of the accelerometer is 78 mV/g and 102 mV/g for X and Y axis respectively with a minimum detectable acceleration of 25 milli-g. Though the prototype uses a perfect de-coupling mechanism, the sensor is quite sensitive off-axially due to asymmetric manual assembly. This can be improved further by the design of the compliant suspension. This and other improvements will be taken up in our future work to establish spring steel as a viable material for meso-scale applications.

Acknowledgement

We thank Mr. G. Ramu for helping us with the wire-cut EDM process and the CNC machining process in fabricating the device.

References

[1] C. H. Liu, A. M. Barzilai, J. K. Reynolds, A. Partridge, T. W. Kenny, J. D. Grade, and H. K. Rockstad, "Characterization of a High-Sensitivity

Micromachined Tunneling Accelerometer with Micro-g Resolution", Journal of Microelectromechanical Systems, Vol. 7, No. 2 (1998) pp. 235–44.

[2] C. Yeh and K. Najafi, "CMOS interface circuitry for a low voltage micromachined tunneling accelerometer", Journal of microelectromechanical systems, Vol. 7, No. 1, March 1998, pp. 6–14.

[3] R. L. Kubena, G. M. Atkinson, W. P. Robinson, and F. P. Stratton, "A New Miniaturized Surface Micromachined Tunneling Accelerometer", IEEE Electron Device Letters, Vol. 17, No. 6 (1996), pp. 306–308.

[4] E. B. Cooper, E. R. Post, S. Griffith, M. A. Schmidt, and C. F. Quate, "A High-resolution Micromachined Interferometric Accelerometer," Applied Physics Letters, Vol. 76, No. 22, 2000, pp. 3316-3318.

[5] N. C. Loh, M. A. Schmidt, and S. R. Manalis, "Sub-10 cm^3 Interferometric Accelerometer with Nano-g Resolution," Journal of Microelectromechanical Systems, Vol. 11, No. 3, 2002, pp. 182–187.

[6] K. J. Ma, N. Yazdi, and K. Najafi, "A bulk-silicon capacitive microaccelerometer with built-in over-range and force feedback electrodes," Tech. Dig. Solid-State Sensors and Actuators Workshop, Hilton Head Island, SC, June 1994, pp. 160–163.

[7] J. Chae, H. Kulah, and K. Najafi, "An In-plane High-sensitivity, Low-noise Micro-g Silicon Accelerometer with CMOS Readout Circuitry," Journal of Microelectromechanical Systems, Vol. 13, No. 4, 2004.

[8] J. Chae, H. Kulah, and K. Najafi, "A monolithic three-axis micro-g micromachined silicon capacitive acceleroemter", Journal of Microelectromechanical systems, Vol. 14, No. 2, April 2005, pp. 235–242.

[9] B. V. Amini and F. Ayazi, "Micro-gravity capacitive silicon-on-insulator accelerometers," in Journal of Micromech. Microeng., Vol. 15,no. 11, pp. 2113–2120, Nov. 2005.

[10] P. Monajemi and F. Ayazi, "Design optimization and implementation of a microgravity capacitive HARPSS accelerometer," IEEE Sensors Journal, Vol. 6, no. 1, 2006, pp. 39–46.

[11] D. L. DeVoe, A. Pisano, "A fully surface micromachined piezoelectric acceleroemter", proceedings of the International Conference on solid-state sensors and actuators, Chicago, June-15-16,1997, pp. 1205–1208.

[12] J. Willis and B. D. Jimerson, "A Piezoelectric Accelerometer," Proceedings of the IEEE, Correspondence, 1964, pp. 871–872.

[13] Y. Ning, Y. Loke and G. McKinnon, "Fabrication and characterization of high –g force silicon piezoresistive accelerometers", Sensors and Actuators A, 48 (1998), pp. 105–108.

[14] H. Chen, M. Bao, H. Zhu and S. Shen, "A piezoresistive accelerometer with a novel vertical beam structure", Sensors and Actuators A. Vol. 63, September 1997, pp. 19–25.

[15] J. H. Sim, C. S. Cho, J. S. Kim, J. H. Lee and J. H. Lee, "Eight-beam piezoresistive accelerometer fabricated by using a selective porous-silicon etching method", Sensors. Actuators A 66 (1998), pp. 273–278.

[16] D. W. Burns, R. D. Horning, W. R. Herb, J. D. Zook, and H. Guckel, "Resonant microbeam accelerometers," Tech. Dig. 8th Int. Conf. on Solid-State Sensors and Actuators (Transducers' 95), Stockholm, Sweden, June 1995, pp. 659–662.

[17] T. A. Roessig, R. T. Howe, A. P. Pisano, and J. H. Smith, “Surface micromachined resonant accelerometer,” Tech. Dig. 9th Int. Conf. Solid-State Sensors and Actuators (Transducers’97), Chicago, IL, June 1997, pp. 859–862.
[18] C. Pedersen and A. Seshia, 2004, “On the optimization of compliant force amplifier mechanisms for surface micromachined resonant accelerometers”, Journal of Micromechanics and Microengineering, Vol. 14, No. 10, pp. 1281–1293.
[19] X. P. S. Su and H. S. Yang, 2001, “Two-stage compliant micro-leverage mechanism optimization in a resonant accelerometer”, Structural and Multidisciplinary Optimization, Vol. 22, pp. 328–336.
[20] A. B. Bhaskar, Girish Krishnan, N. Shamsudhin, and G.K. Ananthasuresh, “Design, Fabrication, and Testing of a Meso-scale Accelerometer Made of Spring Steel,” Journal of the Instrumentation Society of India, Vol. 39, No. 1, March 2009, pp. 46-52.
[21] S. Awtar, “Synthesis and Analysis of Parallel Kinematic XY Flexure Mechanisms,” PhD Thesis, Massachusetts Institute of Technology, Cambridge, MA, 2004.
[22] SolidWorks: 3D CAD Design Software, www.solidworks.com.
[23] COMSOL: Multiphysics Modeling and Simulation, www.comsol.com.
[24] “A1391, A1392, A1393, and A1395: Micro Power 3 V Linear Hall-effect Sensor ICs withTri-State Output and User-Selectable Sleep Mode” data sheet, Allegro Microsystems, Inc.
[25] “LIS3L02AS4: MEMS Inertial Sensor - 3-axis ±2g / ±6g linear accelerometer”, data sheet, STMicroelectronics, 2005.